University of Nebraska - Lincoln

DigitalCommons@University of Nebraska - Lincoln

Peter Dowben Publications   Research Papers in Physics and Astronomy

2014

The unoccupied electronic structure characterization of hydrothermally grown ThO$_2$ single crystals

T D. Kelly
Air Force Institute of Technology, Tony.Kelly@afit.edu

J C. Petrosky
Air Force Institute of Technology, James.Petrosky@afit.edu

D Turner
Oak Ridge Institute for Science and Education

J W. McClory
Air Force Institute of Technology

J M. Mann
Air Force Institute of Technology

See next page for additional authors

Follow this and additional works at: http://digitalcommons.unl.edu/physicsdowben

Part of the Physics Commons

Authors

T D. Kelly, J C. Petrosky, D Turner, J W. McClory, J M. Mann, J W. Kolis, Xin Zhang, and Peter A. Dowben

The unoccupied electronic structure characterization of hydrothermally grown ThO₂ single crystals

T. D. Kelly[*, 1], **J. C. Petrosky**[**, 1]**, D. Turner**[2]**, J. W. McClory**[1]**, J. M. Mann**[3]**, J. W. Kolis**[4]**, Xin Zhang**[5]**, and P. A. Dowben**[5]

[1] Department of Engineering Physics, Air Force Institute of Technology, 2950 Hobson Way, WPAFB, OH 45433, USA
[2] Oak Ridge Institute for Science and Education, 1299 Bethel Valley Road, Oak Ridge, TN 37830, USA
[3] Sensors Directorate, Air Force Research Laboratory, Wright-Patterson AFB, OH 45433, USA
[4] Department of Chemistry and Center for Optical Materials Science and Engineering Technologies (COMSET), Clemson University, Clemson, SC 29634-0973, USA
[5] Department of Physics and Astronomy, Theodore Jorgensen Hall, 855 North 16th Street, University of Nebraska-Lincoln, Lincoln, NE 68588-0299, USA

* Corresponding author: e-mail Tony.Kelly@afit.edu, Phone: +1 937 255 3636 ext 7300, Fax: +1 937 656 6000
** e-mail James.Petrosky@afit.edu

Single crystals of thorium dioxide ThO₂, grown by the hydrothermal growth technique, have been investigated by ultraviolet photoemission spectroscopy (UPS), inverse photoemission spectroscopy (IPES), and L₃, M₃, M₄, and M₅ X-ray absorption near edge spectroscopy (XANES). The experimental band gap for large single crystals has been determined to be 6 eV to 7 eV, from UPS and IPES, in line with expectations. The combined UPS and IPES, place the Fermi level near the conduction band minimum, making these crystals n-type, with extensive band tailing, suggesting an optical gap in the region of 4.8 eV for excitations from occupied to unoccupied edge states. Hybridization between the Th 6d/5f bands with O 2p is strongly implicated.

1 Introduction It is often stated that Th has no 5f electrons and instead adopts the electronic configuration [Rn]6d²7s². This is an extension of the idea that there are no occupied Th valence states when Th is a cation Th⁴⁺ in a compound such as ThO₂. In this scheme, the valence maximum is dominated by O 2p character, as a result of the transfer of the outer Th $6d^2 7s^2$ electrons to the O 2p bands below the valence band maximum (VBM). There exists, however, a body of literature that suggests hybridization between Th and O in ThO₂ which results in valence bands with Th 5f (and/or 6d) character mixing with the O 2p. This results in a fluorite structure that is not purely ionic and possesses some covalent properties.

Theory does tend to suggest hybridization of Th 5f (and/or 6d) with O 2p [1–4]. The manner in which the f-band is included does have a profound effect on the theoretical calculations. For example, a fixed f-band does not result in hybridization [1]. However, resonant photoemission experiments do support hybridization [5].

Like most f systems, the extent of band itinerancy is central to understanding the degree of hybridization, even in the case of a wide band gap insulator like ThO₂. The expectations regarding the ThO₂ band gap vary: theoretical calculations predict a band gap over an extensive range of 4.43 [6], 4.5 [2], 4.673 [4], 4.7 [2], 4.82 [3], 5.0 [5], and 6.9 eV [2]. Some of the variety in the calculated band gap depends upon the functional, e.g. in [2], the different functionals (LDA, LDA + U, and B3LYP) result in the different band gaps of 4.5 eV, 4.7 eV, and 6.9 eV, respectively. Experimental work suggest that the band gap is between 5.0 eV [5] and 6.0 eV [4, 6–8].

Obtaining ThO₂ single crystals by the hydrothermal technique opens a route to resolving questions regarding the electronic structure by enabling spectroscopic meas-

Wiley Online Library

urements of both the occupied and unoccupied band structure. The work of [9, 10] indicates this growth process to be an excellent means of obtaining large single crystals of refractory oxides on the order of several mm. Starting with large single crystals of ThO_2, on the order of 9 mm^2 per face, the electronic structure in the region of the band gap has been probed. As reported here, the occupied and unoccupied band structure was investigated by ultraviolet photoemission spectroscopy and inverse photoemission spectroscopy then compared to X-ray absorption near edge spectroscopy.

2 Methodology The ThO_2 single crystals were synthesized in supercritical CsF mineralizer solutions. The crystal structure was confirmed by XRD and then through the rocking curves, oriented in the (200) direction, as found in other Ref. [9–12]. Before analysis, the crystals were cleaned using an organic solution of mixed crown ethers and picric acid. After cleaning, the crystals were baked in a vacuum desiccator for approximately 16 hours at 180 °C. Details related to the method are to be published elsewhere.

The X-ray absorption near edge spectroscopy (XANES) was measured at the Center for Advanced Microstructures and Devices (CAMD). Thorium L-edge XANES was collected on the wiggler double crystal monochromator (WDCM) beamline in fluorescence mode using a multichannel high purity Ge detector. Thorium M-edge XANES was collected in fluorescence mode on the DCM beamline using a single channel Si detector. All data were collected at room temperature. The XANES data were analyzed with the ATHENA software [13], as detailed elsewhere [14, 15].

XANES cannot be quantified in the same manner as extended absorption fine structure spectroscopy (EXAFS). However, an *ab initio* Green's functions analysis can be done via FEFF 9 code [16, 17], and the spectra can be compared to inverse photoemission, as both probe the unoccupied density of states (DOS). The FEFF 9 software uses a relativistic Green's functions formalism and realizes a self-consistent, real-space multiple scattering mechanism [16–19].

Ultraviolet photoemission spectroscopy (UPS) and inverse photoemission spectroscopy (IPES) experiments were conducted under ultrahigh vacuum conditions (10^{-10} Torr). The UPS technique was conducted using the He(I) 21.2 eV emission line. Photoelectrons were measured with a hemispherical analyzer with a system resolution of 100 meV. The IPES spectra were obtained in the isochromat mode using a variable low energy electron gun. A Geiger–Müller tube, with $I_2(g)$ plus He, was used to detect the electron generated photon emission and the IPES spectra were limited by an instrumental linewidth of approximately ~400 meV, as described elsewhere [20, 21]. The binding energies are all referenced with respect to the Fermi level (E_F) of a reference Au foil, and reported as $E–E_F$, making occupied state energies negative. While no

sample charging effects were observed, charging and final state effects cannot be completely excluded from the photoemission measurements.

3 X-ray absorption near edge spectroscopy (XANES) In Fig. 1, the experimental Th L_3 XANES spectrum is plotted along with various theoretical XANES spectra. Multiple calculations were made with increasingly larger full multiple scattering spheres until the model XANES converged. The full multiple scattering spheres ranged in size from the smallest sphere containing 8 atoms at a radius 3 Å to the largest full multiple scattering containing 121 atoms at a radius of 7.5 Å (one more than is shown in Fig. 1). The starting point, i.e. the bottom spectrum in Fig. 1 (μ_0), is the smoothly varying background for a free Th atom. Moving up in Fig. 1, the right-hand side indicates the number of additional atoms and of what species are added into the model cluster, with increasing cluster size. We observe that the XANES calculations converge relatively quickly after adding 32 O and 12 Th atoms to the cluster at a full multiple scattering radius of 5.0 Å.

All the calculations discussed later are based upon a cluster with a full multiple scattering sphere radius of 7.0 Å, and thus the local electronic DOS are the result of considering cluster sizes of approximately 99 atoms. With nearly 100 atoms in the cluster, the calculations are considered more reliable for the FEFF 9 Green's function formalism. A Hedin–Lundqvist self-energy was used for the energy dependent exchange correlation potential and the ground state potential was used to calculate the background, but the f-electrons were unconstrained.

The experimental data obtained at four different Th edges (L_3, M_3, M_4, and M_5) are plotted in Fig. 2. The data have been shifted by E_0, core level binding energy. This has the added benefit of being able to compare to the local electronic DOS, associated with unoccupied states, particularly the d states (example [22]). The Th white line
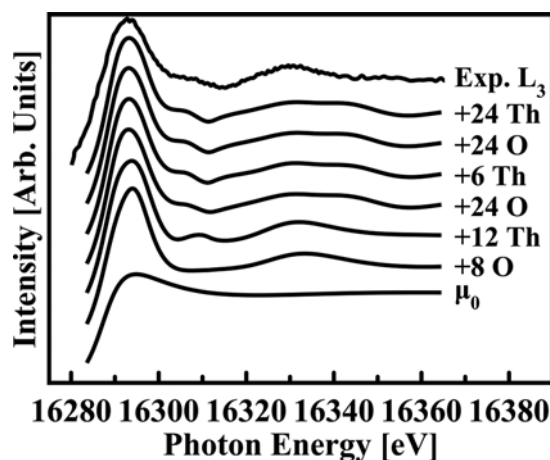

Figure 1 Theoretical Th L_3-edge XANES spectra calculated with increasingly larger full multiple scattering shells, from bottom to top (see text). The top spectrum is the normalized experimental data.
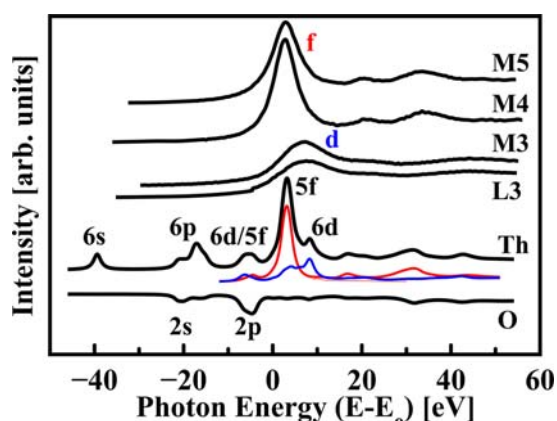
Figure 2 Experimental XANES spectra for the L_3, M_3, M_4, and M_5 edges, as labeled. The calculated total local DOS for both thorium (Th) and oxygen (O) have been plotted (black, as labeled) along with the partial Th local 5f (red line) and 6d (blue line) DOS. The oxygen DOS has been inverted for ease of identification.

(sharp rising edge extending beyond the photoelectric edge) is compared to the Green's function calculations in a similar approach. A similar experiment was performed with amorphous actinide compounds in [23].

From the dipole selection rules, the expected transitions at the L_3 and M_3 edges are from states of p to s and d character (p → s and p → d). Likewise, M_4 and M_5 correspond to d → p and d → f transitions. The differences in the p and d edges are apparent in Fig. 2, with the M_4 and M_5 XANES spectra rising sooner and more sharply than the L_3 and M_3 edges. The similarity between the XANES data taken at the M_4 and M_5 Th edges reflect the dominant d → 5f transitions and the placement of the 5f-type electron states just above the Fermi level or at the bottom of the conduction band. The similarity between the data taken at L_3 and M_3 is also expected and reflects the $2p_{3/2}$ and $3p_{3/2}$ → 6d transitions and the placement of the d-type electrons, $2p_{3/2}$ and $3p_{3/2}$, respectively. Comparatively, M_4 and M_5 Th edges correspond to 6d-weighted electron states at energies farther above the Fermi level than is the case for the 5f states, well above the bottom of the conduction band minimum. This assignment for the unoccupied states is consistent with our theoretical expectations and the LDA + U calculations of [2].

In Fig. 2, the calculated total local DOS have been plotted (black line) below the experimental data, broadened with a Lorentzian by 1.0 eV half-width at half-maximum (HWHM). The total Th local DOS is plotted as the upper black line, whereas the total O local DOS have been inverted for ease of comparison with the Th DOS. The partial Th local 5f (red line) and 6d (blue line) DOS have been plotted. This partial angular momentum projected local DOS also indicates that the d-character states sit at higher energies than those of f-character, consistent with the experimental results. We find that while there is only a very small amount of unoccupied O 2p weight,

some Th and O s-character local DOS is unoccupied, generally at higher energies than both Th f and d. Generally, the experimental data are well described by the Green's function calculations and the LDA + U calculation found in [2].

While the unoccupied band structure is composed primarily of the 5f and 6d bands, with the 5f band just above the band gap, consistent with prior theory [2–6], hybridization is implicated in the Th 6d, 5f band mixing with the occupied O 2p states and Th 6p with the O 2s. This hybridization indicates some covalency in ThO_2 and implies that the pure ionic model is not the correct approach. The *ab initio* total charge transfer calculated is about $0.584e$ on Th and $–0.293e$ on O, as opposed to purely ionic $+4e$ and $–2e$ respectively. The similarity of the XANES unoccupied Th 6d weighted spectra (L_3 and M_3 of Fig. 2) with the inverse photoemission, support this contention as well.

4 UPS and IPES characterization The UPS and IPES spectra have been plotted together in Fig. 3. The O 2p weighted DOS is apparent at approximately 5 eV below the Fermi level, matching well the DOS plotted in Fig. 2. The vertical binding energy of the unoccupied 5f/6d states start at 1–2 eV above the Fermi level. This places the measured band gap between 6–7 eV, close to the estimated values of 5.0 eV [5], and 6.9 eV [2], and in general agreement with the expected prior experimental values of 5.0 eV to 6.0 eV [4–8]. Given that density functional theory usually underestimates the band gap, the fact that most theory obtains values for the band gap that are less than measured here is not too surprising, although the DFT hybrid functional estimate for the band gap (6.9 eV [2]) is very close to the experimental estimates obtained here.

The unoccupied conduction band tail DOS, probed by IPES, starts at approximately 0.9 ± 0.4 eV above the Fermi level, while the O 2p weighted DOS band tail extends to approximately 3.9 ± 0.2 eV, below the Fermi level, so that band gap, inclusive of the rather extensive band tail states, is smaller than the previously published band gaps, i.e.
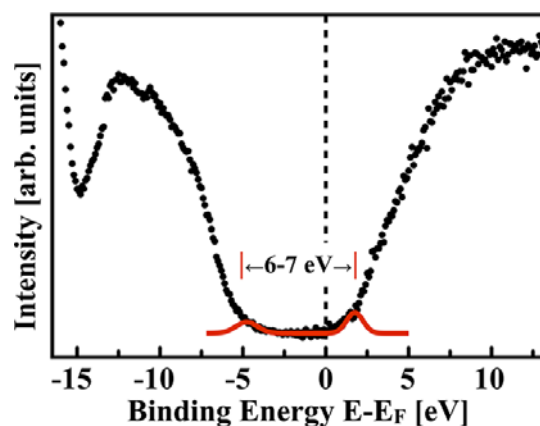

Figure 3 Ultraviolet photoemission (left) and inverse photoemission (right) spectra referenced ThO_2. Binding energies are referenced to the Fermi level as $E–E_F$.

here it is about 4.8 ± 0.4 eV. This suggests that the optical gap may be quite broad and significantly smaller than the ground state band gap. This narrowing of the band gap is possibly a result of a heterogeneous mixture of defects states and surface effects. Otherwise, the inverse photo-emission determined DOS (Fig. 3) resembles that of the XANES spectra of Figs. 1 and 2, again supporting the con-tention [1–4] that the 5f/6d and O 2p states hybridize. Hence the electronic structure, away from the band edge tail states, is dominated by a hybridized band structure rather than localized, narrow width, isolated non-dispersive 5f/6d states. The photoemission resembles the spectra ob-tained for the fluorite phase Gd:HfO$_2$ alloys, with a very similar DOS [24], including extensive tail states at the va-lence band maximum.

As the placement of the Fermi level does not lie in the center of the gap, but rather lies closer to the conduction band edge, the combined photoemission and inverse pho-toemission indicate that our ThO$_2$ crystals are n-type. This could occur for a number of reasons, including (1) surface oxygen vacancies, (2) impurities from the growth process have diffused into the ThO$_2$ acting as donors, (3) Th inter-stitials and O vacancies in the crystal act as donor sites, (4) or the creation of anti-Frenkel point defects, the latter con-dition is expected in these fluorite structure crystals based upon DFT calculations [25, 26]. Further studies, including defect analysis by non-destructive techniques, are needed.

5 Conclusions Single crystals of ThO$_2$ have been in-vestigated to characterize the valence and conduction band structure in the vicinity of the band gap. There is hybridi-zation between the occupied Th 6d and Th 5f bands with the O 2p, resulting in only partial Th–O charge transfer, in spite of the 6 eV to 7 eV band gap. This determination does not account for charging, and the measurement here should be considered an upper bound. Similarly, the unoc-cupied states, just above the Fermi level, are dominated by a hybridized band structure rather than localized, narrow width, isolated non-dispersive 5f/6d states. These crystals appear n-type, suggesting the presence of a small amount of O point defects, consistent with the long band tails.

References

[1] P. J. Kelly and M. S. S. Brooks, J. Chem. Soc. Faraday Trans. **2**(83), 1189 (1987).

[2] B. Szpunar and J. A. Szpunar, J. Nucl. Mater. **439**, 243 (2013).

[3] R. Terki, H. Feraoun, G. Bertrand, and H. Aourag, Comput. Mater. Sci. **33**, 44 (2005).

[4] B.-T. Wang, H. Shi, W.-D. Li, and P. Zhang, J. Nucl. Mater. **399**, 181 (2010).

[5] W. P. Ellis, A. M. Boring, J. W. Allen, L. E. Cox, R. D. Cowan, B. B. Pate, A. J. Arko, and I. Lindau, Solid State Commun. **72**, 725 (1989).

[6] A. Boudjemline, L. Louail, M. M. Islam, and B. Diawara, Comput. Mater. Sci. **50**, 44 (2011).

[7] A. A. Sviridova and N. V. Suikovskaya, Opt. Spectrosc. **22**, 940 (1965).

[8] B. Szpunar and J. A Szpunar, J. Phys. Chem. Solids **74**, 1632 (2013).

[9] M. Mann, D. Thompson, K. Serivalsatit, T. M. Tritt, J. Bal-lato, and J. Kolis, Cryst. Growth Des. **10**, 2146 (2010).

[10] M. Mann and J. Kolis, J. Cryst. Growth **312**, 461 (2010).

[11] J. Castilow, T. W. Zens, J. M. Mann, J. W. Kolis, C. D. McMillen, and J. C. Petrosky, Mater. Res. Soc. Symp. Proc. **1576**, (2013).

[12] T. D. Kelly, J. C. Petrosky, J. W. McClory, T. W. Zens, D. Turner, J. M. Mann, J. W. Kolis, J. A. C. Santana, and P. A. Dowben, Mater. Res. Soc. Symp. Proc. **1576**, DOI 10.1557/opl.2013.996 (2013).

[13] B. Ravel and M. Newville, J. Synchrotron Radiat. **12**, 537 (2005).

[14] J. Liu, G. Luo, W.-N. Mei, O. Kizilkaya, E. D. Shepherd, J. I. Brand, and P. A. Dowben, J. Phys. D, Appl. Phys. **43**, 085403 (2010).

[15] T. D. Kelly, L. Kong, D. A. Buchanan, A. T. Brant, J. C. Pe-trosky, J. W. McClory, V. T. Adamiv, Y. V. Burak, and P. A. Dowben, Phys. Status Solidi B **250**, 1376 (2013).

[16] J. J. Rehr, J. J. Kas, M. P. Prange, A. P. Sorini, Y. Taki-moto, and F. Vila, C. R. Physique **10**, 548 (2009).

[17] J. J. Rehr, J. J. Kas, F. D. Vila, M. P. Prange, and K. Joris-sen, Phys. Chem. **72**, 621 (2000).

[18] A. L. Ankudinov, B. Ravel, J. J. Rehr, and S. D. Conradson, Phys. Rev. B **58**, 7565 (1998).

[19] J. J. Rehr and R. C. Albers, Rev. Mod. Phys. **72**, 621 (2000).

[20] J. Zhang, D. N. McIlroy, P. A. Dowben, H. Zeng, G. Vidali, D. Heskett, and M. Onellion, J. Phys.: Condens. Matter **7**, 7185 (1995).

[21] D. N. McIlroy, J. Zhang, P. A. Dowben, and D. Heskett, Mater. Sci. Eng. A **217–218**, 64 (1996).

[22] J. Graetz, C. C. Ahn, H. Ouyang, T. Zens, P. Rez, and B. Fultz, Phys. Rev. B **69**, 235103 (2004).

[23] J. Petiau, G. Calas, D. Petit-Maire, A. Bianconi, M. Ben-fatto, and A. Macrelli, Phys. Rev. B **34**, 7350 (1986).

[24] Ya. B. Losovyj, I. Ketsman, A. Sokolov, K. D. Be-lashchenko, P. A. Dowben, J. Tang, and Z. Wang, Appl. Phys. Lett. **91**, 132908 (2007).

[25] Y. Lu, Y. Yang, and P. Zhang, J. Phys.: Condens. Matter **24**, 335801 (2012).

[26] R. K. Behera and C. S. Deo, J. Phys.: Condens. Matter **24**, 215405 (2012).